

# Adsorption of Fluorocarbons and Chlorocarbons by Highly Porous and Robust Fluorinated Zirconium Metal–Organic Frameworks

Hao Wang,<sup>\*,†</sup> Liang Yu,<sup>†</sup> Yuhan Lin,<sup>†</sup> Junjie Peng, Simon J. Teat, Lawrence J. Williams, and Jing Li<sup>\*</sup>

 Cite This: *Inorg. Chem.* 2020, 59, 4167–4171

 Read Online

ACCESS |

 Metrics & More

 Article Recommendations

 Supporting Information

**ABSTRACT:** Fluorocarbons and chlorocarbons are common volatile organic compounds that pose serious risk to the environment and human health and therefore need to be effectively captured. Herein, we report a series of highly fluorinated metal–organic frameworks with high porosity (Brunauer–Emmett–Teller surface area  $\sim 3000$  m<sup>2</sup>/g) and stability. They show exceptionally high capacity and good recyclability toward the adsorption of fluorocarbons and chlorocarbons.

Metal–organic frameworks (MOFs) are particularly attractive for their potential use in molecular adsorption and capture in light of their high porosity, tunable pore structure, and functionality.<sup>1–6</sup> While fluorinated MOFs are appealing as adsorbents for the adsorption and capture of fluorocarbons and chlorocarbons because of their fluorophilic character and resistance toward moisture,<sup>7,8</sup> their preparation is generally challenging especially for those with high porosity.<sup>9–14</sup> A few fluorinated MOFs with high porosity have been reported; however, the syntheses of fluorine-rich organic ligands are rather complicated and often air-sensitive, which can often be accomplished only under an inert atmosphere such as inside a glovebox. In addition, activation of these MOFs is usually quite difficult because they generally suffer from fragile structures.<sup>15</sup>

Over the past decade, the emerging zirconium-based MOFs (Zr-MOFs) have largely addressed the stability issue. Having relatively strong Zr–O bonds and robust hexanuclear inorganic building units, Zr-MOFs show significantly enhanced thermal and moisture resistance, with some of which approaching the stability level of traditional inorganic adsorbents.<sup>16–20</sup> This suggests that, guided by reticular chemistry, Zr-MOFs with high porosity, stability, and fluorophilicity that are specifically suitable for capture of fluorocarbons and chlorocarbons may well be achievable. In this context, we use highly fluorinated organic linkers to construct Zr-MOFs in order to (1) increase their hydrophobicity and consequently their resistance toward moisture and (2) enhance their interaction with fluorocarbons and chlorocarbons. As expected, the Zr-MOFs synthesized using these ligands exhibit strong hydrophobicity and possess the highest porosity among all fluorinated MOFs reported to date. Also, they display high adsorption capability toward fluorocarbons and chlorocarbons.

Guided by reticular chemistry, we have successfully constructed three robust Zr-MOFs having the same metal building unit (Zr<sub>6</sub>), connectivity (12), and structural topology (fcu). The three fluorinated dicarboxylic acids used to build these structures, H<sub>2</sub>tpdc-F<sub>4</sub>, H<sub>2</sub>tpdc-(CF<sub>3</sub>)<sub>2</sub>, and H<sub>2</sub>qpdc-F<sub>8</sub> (Figure 1), were synthesized through Suzuki coupling reactions between fluorinated phenyl or biphenyl fragments and 4-

methoxycarbonylphenylboronic acid (see the Supporting Information for the detailed synthesis of organic ligands). Solvothermal reactions between zirconium salts (ZrCl<sub>4</sub> or ZrOCl<sub>2</sub>·8H<sub>2</sub>O) and the corresponding organic ligands in *N,N*-dimethylformamide with the addition of benzoic acid or acetic acid as modulators yielded three new compounds with formulas of Zr<sub>6</sub>O<sub>4</sub>(OH)<sub>4</sub>(tpdc-F<sub>4</sub>)<sub>6</sub> (1), Zr<sub>6</sub>O<sub>4</sub>(OH)<sub>4</sub>(tpdc-(CF<sub>3</sub>)<sub>2</sub>)<sub>6</sub> (2), and Zr<sub>6</sub>O<sub>4</sub>(OH)<sub>4</sub>(qpdc-F<sub>8</sub>)<sub>6</sub> (3), respectively (see the experimental section for the detailed synthesis of MOFs). The materials were obtained as octahedral crystals (Figure S4).

Single-crystal X-ray diffraction analysis reveals that all three compounds crystallize in the cubic crystal system with space groups of *Fm* $\bar{3}$ *m* for compounds 1 and 2 and *Fd* $\bar{3}$ *m* for compound 3 (see Tables S1–S3 for detailed crystallographic data). All three compounds feature connectivity similar to that of the UiO family.<sup>18</sup> They are built on 12-connected hexanuclear units, Zr<sub>6</sub>O<sub>4</sub>(OH)<sub>4</sub>(COO)<sub>12</sub>, which are propagated through organic linkers, forming three-dimensional frameworks with fcu topology. Similar to other fcu-type compounds, the structure contains two types of cages with tetrahedral and octahedral geometries that are decorated by fluorine atoms from the organic ligands (Figure 1). Defects (missing linkers) are commonly observed for UiO-type Zr-MOFs and are observed in these compounds also. For compound 3, which has the highest defect ratio (27%) among the three compounds, a defect model was used for refinement of its structure, where the ligands missing are replaced by water.

The phase purities of the Zr-MOFs have been confirmed by powder X-ray diffraction (PXRD) analysis (Figures S6–S8). Thermogravimetric analysis (TGA) reveals that compounds

Received: January 4, 2020

Published: March 18, 2020

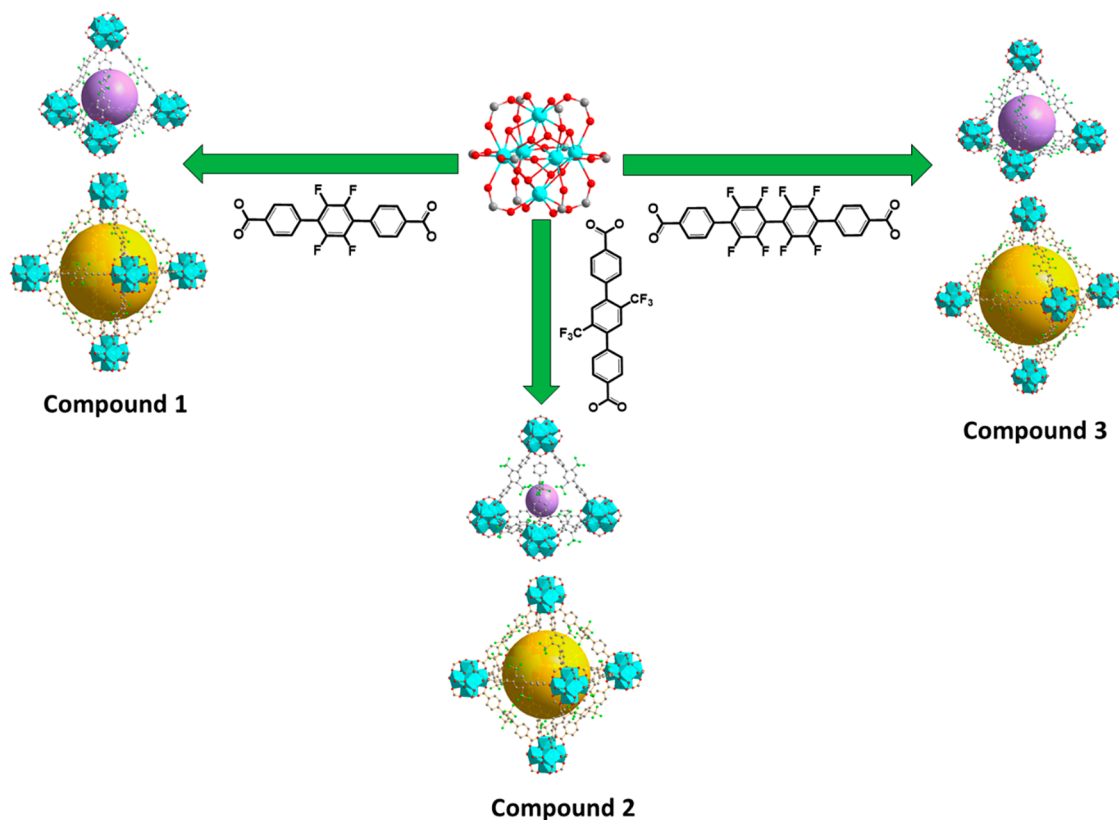


**Figure 1.** Construction of compounds 1–3. Color code: Zr, cyan polyhedra; O, red; C, gray; F, green. Hydrogen atoms are omitted for clarity.

1–3 lose weight below 200 °C and reach a plateau before 400–500 °C, indicating high thermal stability (Figures S9–S11). The amount of weight loss is 40%, 10%, and 30% for 1–3, respectively. Previous studies have shown that fluorinated-ligand-based Cu-MOFs suffer from relatively lower thermal stability as a consequence of the weaker metal–ligand coordination.<sup>15</sup> However, this is not the case for the title compounds because their structures are built on robust Zr<sub>6</sub> secondary building units with strong metal–ligand coordination as well as high connectivity. The decomposition temperatures of compounds 1–3 are comparable to those of nonfluorinated analogues.<sup>21</sup> The notably smaller weight loss of compound 2 compared to the other two analogous structures suggests its higher hydrophobicity. This has been commonly observed for hydrophobic MOFs that are synthesized in hydrophilic solvents.<sup>22</sup> It is also noteworthy that the activated sample of compound 2 shows essentially no weight gain upon exposure to air for 2 days (Figure S12), suggesting that it does not adsorb any water from air. A parallel experiment was carried out to compare the relative hydrophobicity of the three compounds: when 20 mg of each sample was dispersed in 5 mL of water for 10 h, compounds 1 and 3 partially settled down at the bottom of the vial, while compound 2 remained floating at the surface of water (Figure S13). This is consistent with the TGA results and confirms the superior hydrophobicity of compound 2. This behavior is not surprising because the trifluoromethyl functional groups render additional hydrophobicity to the framework, which has been demonstrated in other trifluoromethyl-functionalized MOFs.<sup>23</sup> To quantitatively assess the hydrophobicity of compound 2, we performed water adsorption measurements. As expected, this material

shows negligible water adsorption despite its exceptional porosity, confirming its hydrophobic nature (Figure S14).

Nitrogen sorption measurements were performed at 77 K to evaluate the porosity of these materials. The saturated uptake of nitrogen for compounds 1–3 are 12, 31, and 34 mmol/g, yielding Brunauer–Emmett–Teller (BET) surface areas of 1012, 2819, and 3108 m<sup>2</sup>/g and pore volumes of 0.42, 1.06, and 1.11 cm<sup>3</sup>/g, respectively (Figures 2 and S15 and S16). The

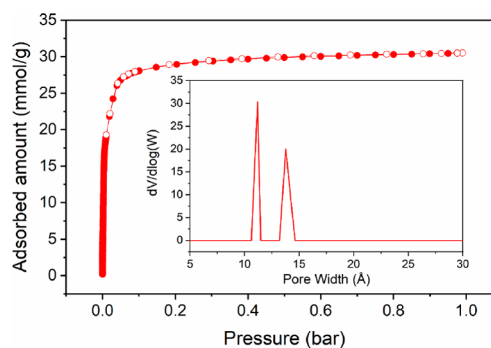


**Figure 2.** Nitrogen adsorption–desorption isotherms at 77 K for compound 2. The inset shows the pore-size distribution.

obviously lower porosity for compound 1 may be attributed to incomplete activation and partial structural degradation upon heating, as confirmed by the broadened peaks of the PXRD pattern of the activated sample (Figure S6). Tremendous efforts have been made to optimize the activation conditions for compound 1. However, it appears that its stability is noticeably lower than that of the other two compounds. Its structure is fragile and tends to collapse upon guest removal. In

addition, the presence of defects is not leading to a decrease in the structural stability or appearance of noticeable mesoporosity. The BET surface areas of compounds **2** and **3** are comparable to those of other reported UiO-68 analogues with similar structural connectivity.<sup>21</sup> The values are, to the best of our knowledge, the highest among all fluorinated porous materials reported to date.<sup>15</sup> The density functional theory pore-size distribution from nitrogen adsorption isotherms reveals that compounds **2** and **3** possess two types of pores, with diameters of 11 and 16 Å for compound **2** and 13 and 18 Å for compound **3**. This is consistent with their crystal structures, which possess a smaller tetrahedral cage and a larger octahedral cage.

Because of its high porosity and exceptional hydrophobicity, exploration of the adsorption of fluorocarbons and chlorocarbons has been focused on compound **2**. The adsorption measurements have been evaluated with representative fluorocarbons and chlorocarbons molecules: perfluorohexane (PFH), trichloroethylene (TCE), and perchloroethylene (PCE). PFH is a greenhouse species with a 100-year global warming potential (GWP) that is 3–4 orders of magnitude higher than that of carbon dioxide.<sup>24</sup> It is widely used in industry for the electronic cooling process. PCE and TCE are widely used as solvents for processes such as metal degreasing, dry cleaning, and the manufacture of plastics. Through leakage and spillage, they are released to the environment and are regarded as two of the most ubiquitous groundwater contaminants, and their toxicity and persistence are of great concern.<sup>25,26</sup>

The adsorption experiments were performed with a homemade gravimetric adsorption analyzer modified from a Q50 unit (TA Instruments).<sup>27</sup> The adsorption capacity was measured at 30 °C with partial pressures of 150, 50, and 15 Torr for PFH, TCE, and PCE, respectively. As shown in Figure 3, the adsorption capacities for PFH, TCE, and PCE are 142, 108, and 143 wt % for **2**, respectively. The adsorption is fast and reaches saturation within a couple of minutes. Material stability toward the adsorption–desorption process was evaluated by a cycle test. After 10 repeated adsorption–desorption cycles, the adsorption capacity of PCE on compound **2** remains the same, indicating high stability of the material (Figures 4 and S7). To investigate how the partial pressure of the adsorbate would affect the adsorption capacity, we have performed an adsorption experiment at lower concentration. The result displays that compound **2** adsorbs 96 wt % of TCE at a partial pressure of 2.5 Torr (Figure S18), only slightly lower than the value at 50 Torr (108 wt %). The adsorbed TCE can be removed completely from the MOF simply by nitrogen purging. To learn whether the trifluoromethyl functionalization is contributing to the high adsorption capacity of compound **2**, we performed adsorption measurements on pristine UiO-68, the parent structure of compound **2**. UiO-68 adsorbs 92 wt % of TCE at 30 °C and 50 Torr, notably lower than that of compound **2** (108 wt %) under identical conditions (Figures S19–S21). Considering the higher surface area of the former (3652 m<sup>2</sup>/g) than that of the latter (2819 m<sup>2</sup>/g), it is fair to conclude that the functionalization of trifluoromethyl groups contributes to the high hydrophobicity of the MOF, which further enhances its adsorption capacity.<sup>23</sup> In addition, we collected the adsorption–desorption isotherm of TCE on compound **2** with a volumetric adsorption analyzer, and the results agree well with the gravimetric adsorption results (Figure S22). Adsorption of

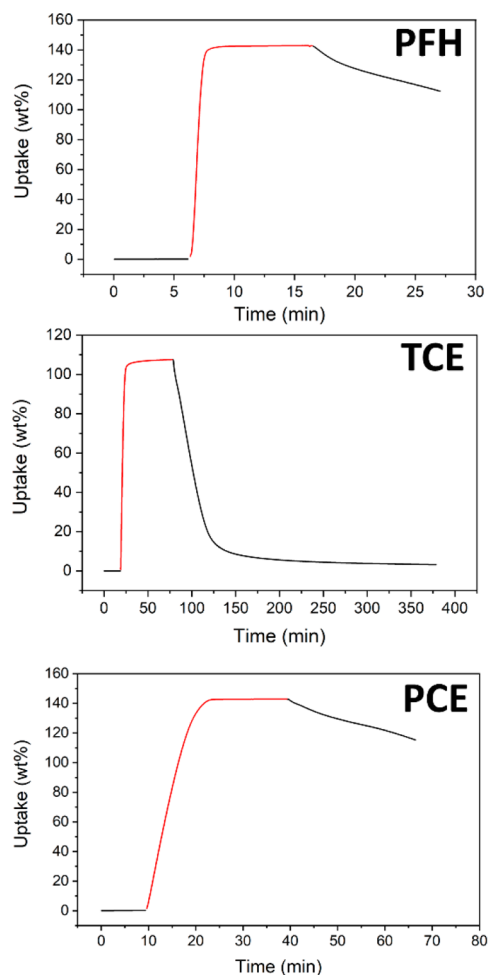


**Figure 3.** Adsorption uptake of the selected fluorocarbons and chlorocarbons for compound **2**. Red and black curves represent data collected under adsorbate vapors and pure nitrogen, respectively.

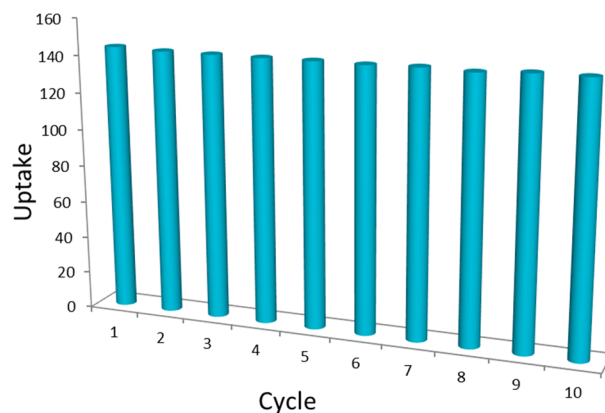


**Figure 4.** Adsorption–desorption cycles of PCE on compound **2**.

the selected fluorocarbons and chlorocarbons on compounds **1** and **3** was also tested (Figure S17). The adsorption capacities of **1** are substantially lower than those of **2** and **3**. This is not surprising because the measured porosity of compound **1** is lower. Compound **3** also exhibits a high adsorption capacity for the selected analytes, which is comparable to that of **2**. It is noteworthy that the amounts of PCE adsorbed in **2** and **3** are the highest among all previously reported adsorbents (Table S4).<sup>28–31</sup>

In summary, we have demonstrated the utilization of reticular chemistry on fcu Zr-MOFs to develop fluorinated MOFs with high stability and porosity. The materials obtained show high adsorption capability toward fluorocarbons and chlorocarbons and are fully recyclable. This strategy can be used for the development of fluorinated MOFs with tailored pore structures for the effective capture of targeted molecules.

## ■ ASSOCIATED CONTENT

### SI Supporting Information

The Supporting Information is available free of charge at <https://pubs.acs.org/doi/10.1021/acs.inorgchem.0c00018>.

Detailed synthesis of organic ligands, crystal images of MOFs, crystal data and structure refinement of MOFs, PXRD and TGA results of MOFs, water adsorption isotherm of compound 2, porosity characterization of MOFs, and adsorption of the selected fluorocarbons and chlorocarbons on MOFs (PDF)

### Accession Codes

CCDC 1910170–1910172 contain the supplementary crystallographic data for this paper. These data can be obtained free of charge via [www.ccdc.cam.ac.uk/data\\_request/cif](http://www.ccdc.cam.ac.uk/data_request/cif), or by emailing [data\\_request@ccdc.cam.ac.uk](mailto:data_request@ccdc.cam.ac.uk), or by contacting The Cambridge Crystallographic Data Centre, 12 Union Road, Cambridge CB2 1EZ, UK; fax: +44 1223 336033.

## ■ AUTHOR INFORMATION

### Corresponding Authors

**Hao Wang** – Hoffmann Institute of Advanced Materials, Shenzhen Polytechnic, Shenzhen, Guangdong 518055, China; Department of Chemistry and Chemical Biology, Rutgers University, Piscataway, New Jersey 08854, United States; [orcid.org/0000-0001-7732-778X](https://orcid.org/0000-0001-7732-778X); Email: [wanghao@szpt.edu.cn](mailto:wanghao@szpt.edu.cn)

**Jing Li** – Department of Chemistry and Chemical Biology, Rutgers University, Piscataway, New Jersey 08854, United States; Hoffmann Institute of Advanced Materials, Shenzhen Polytechnic, Shenzhen, Guangdong 518055, China; [orcid.org/0000-0001-7792-4322](https://orcid.org/0000-0001-7792-4322); Email: [jingli@rutgers.edu](mailto:jingli@rutgers.edu)

### Authors

**Liang Yu** – Hoffmann Institute of Advanced Materials, Shenzhen Polytechnic, Shenzhen, Guangdong 518055, China

**Yuhan Lin** – Hoffmann Institute of Advanced Materials, Shenzhen Polytechnic, Shenzhen, Guangdong 518055, China

**Junjie Peng** – School of Chemistry and Chemical Engineering, South China University of Technology, Guangzhou, Guangdong 510641, P. R. China

**Simon J. Teat** – Advanced Light Source, Lawrence Berkeley National Laboratory, Berkeley, California 94720, United States

**Lawrence J. Williams** – Department of Chemistry and Chemical Biology, Rutgers University, Piscataway, New Jersey 08854, United States

Complete contact information is available at: <https://pubs.acs.org/doi/10.1021/acs.inorgchem.0c00018>

### Author Contributions

†These authors contributed equally.

### Notes

The authors declare no competing financial interest.

## ■ ACKNOWLEDGMENTS

We thank the National Natural Science Foundation of China (Grant 21901166) and Guangdong Natural Science Foundation (Grant 2019A1515010692) for financial support. Work in the U.S. was supported by the Materials Sciences and Engineering Division, Office of Basic Research Energy Sciences, U.S. Department of Energy (DOE), through Grant DE-FG02-08ER-46491. This research used resources of the Advanced Light Source, which is a U.S. DOE Office of Science User Facility, under Contract DE-AC02-05CH11231.

## ■ REFERENCES

- (1) Wang, H.; Lustig, W. P.; Li, J. Sensing and capture of toxic and hazardous gases and vapors by metal–organic frameworks. *Chem. Soc. Rev.* **2018**, *47* (13), 4729–4756.
- (2) Canivet, J.; Fateeva, A.; Guo, Y.; Coasne, B.; Farrusseng, D. Water adsorption in MOFs: fundamentals and applications. *Chem. Soc. Rev.* **2014**, *43* (16), 5594–5617.
- (3) Barea, E.; Montoro, C.; Navarro, J. A. R. Toxic gas removal - metal-organic frameworks for the capture and degradation of toxic gases and vapours. *Chem. Soc. Rev.* **2014**, *43* (16), 5419–5430.
- (4) Liao, P.-Q.; Huang, N.-Y.; Zhang, W.-X.; Zhang, J.-P.; Chen, X.-M. Controlling guest conformation for efficient purification of butadiene. *Science* **2017**, *356* (6343), 1193–1196.
- (5) Cui, X.; Chen, K.; Xing, H.; Yang, Q.; Krishna, R.; Bao, Z.; Wu, H.; Zhou, W.; Dong, X.; Han, Y.; Li, B.; Ren, Q.; Zaworotko, M. J.; Chen, B. Pore chemistry and size control in hybrid porous materials for acetylene capture from ethylene. *Science* **2016**, *353* (6295), 141–144.
- (6) Mason, J. A.; Oktawiec, J.; Taylor, M. K.; Hudson, M. R.; Rodriguez, J.; Bachman, J. E.; Gonzalez, M. I.; Cervellino, A.; Guagliardi, A.; Brown, C. M.; Llewellyn, P. L.; Masciocchi, N.; Long, J. R. Methane storage in flexible metal–organic frameworks with intrinsic thermal management. *Nature* **2015**, *527* (7578), 357–361.
- (7) Fernandez, C. A.; Thallapally, P. K.; Motkuri, R. K.; Nune, S. K.; Sumrak, J. C.; Tian, J.; Liu, J. Gas-Induced Expansion and Contraction of a Fluorinated Metal–Organic Framework. *Cryst. Growth Des.* **2010**, *10* (3), 1037–1039.
- (8) Deria, P.; Mondloch, J. E.; Tylianakis, E.; Ghosh, P.; Bury, W.; Snurr, R. Q.; Hupp, J. T.; Farha, O. K. Perfluoroalkane Functionalization of NU-1000 via Solvent-Assisted Ligand Incorporation: Synthesis and CO<sub>2</sub> Adsorption Studies. *J. Am. Chem. Soc.* **2013**, *135* (45), 16801–16804.
- (9) Yang, C.; Wang, X.; Omary, M. A. Fluorous Metal–Organic Frameworks for High-Density Gas Adsorption. *J. Am. Chem. Soc.* **2007**, *129* (50), 15454–15455.
- (10) Yang, C.; Wang, X.; Omary, M. A. Crystallographic Observation of Dynamic Gas Adsorption Sites and Thermal Expansion in a Breathable Fluorous Metal–Organic Framework. *Angew. Chem., Int. Ed.* **2009**, *48* (14), 2500–2505.
- (11) Zheng, J.; Vemuri, R. S.; Estevez, L.; Koech, P. K.; Varga, T.; Camaioni, D. M.; Blake, T. A.; McGrail, B. P.; Motkuri, R. K. Pore-Engineered Metal–Organic Frameworks with Excellent Adsorption of Water and Fluorocarbon Refrigerant for Cooling Applications. *J. Am. Chem. Soc.* **2017**, *139* (31), 10601–10604.
- (12) Annapureddy, H. V. R.; Nune, S. K.; Motkuri, R. K.; McGrail, B. P.; Dang, L. X. A Combined Experimental and Computational Study on the Stability of Nanofluids Containing Metal Organic Frameworks. *J. Phys. Chem. B* **2015**, *119* (29), 8992–8999.
- (13) Motkuri, R. K.; Annapureddy, H. V. R.; Vijaykumar, M.; Schaeff, H. T.; Martin, P. F.; McGrail, B. P.; Dang, L. X.; Krishna, R.; Thallapally, P. K. Fluorocarbon adsorption in hierarchical porous frameworks. *Nat. Commun.* **2014**, *5*, 4368.
- (14) Ji, P.; Drake, T.; Murakami, A.; Oliveres, P.; Skone, J. H.; Lin, W. Tuning Lewis Acidity of Metal–Organic Frameworks via Perfluorination of Bridging Ligands: Spectroscopic, Theoretical, and Catalytic Studies. *J. Am. Chem. Soc.* **2018**, *140* (33), 10553–10561.

- (15) Chen, T.-H.; Popov, I.; Kaveevivitchai, W.; Chuang, Y.-C.; Chen, Y.-S.; Jacobson, A. J.; Miljanić, O. Š. Mesoporous Fluorinated Metal–Organic Frameworks with Exceptional Adsorption of Fluorocarbons and CFCs. *Angew. Chem., Int. Ed.* **2015**, *54* (47), 13902–13906.
- (16) Bai, Y.; Dou, Y.; Xie, L.-H.; Rutledge, W.; Li, J.-R.; Zhou, H.-C. Zr-based metal–organic frameworks: design, synthesis, structure, and applications. *Chem. Soc. Rev.* **2016**, *45*, 2327.
- (17) Wang, H.; Dong, X.; Lin, J.; Teat, S. J.; Jensen, S.; Cure, J.; Alexandrov, E. V.; Xia, Q.; Tan, K.; Wang, Q.; Olson, D. H.; Proserpio, D. M.; Chabal, Y. J.; Thonhauser, T.; Sun, J.; Han, Y.; Li, J. Topologically guided tuning of Zr-MOF pore structures for highly selective separation of C6 alkane isomers. *Nat. Commun.* **2018**, *9* (1), 1745.
- (18) Cavka, J. H.; Jakobsen, S.; Olsbye, U.; Guillou, N.; Lamberti, C.; Bordiga, S.; Lillerud, K. P. A New Zirconium Inorganic Building Brick Forming Metal Organic Frameworks with Exceptional Stability. *J. Am. Chem. Soc.* **2008**, *130* (42), 13850–13851.
- (19) Guillerm, V.; Ragon, F.; Dan-Hardi, M.; Devic, T.; Vishnuvarthan, M.; Campo, B.; Vimont, A.; Clet, G.; Yang, Q.; Maurin, G.; Férey, G.; Vittadini, A.; Gross, S.; Serre, C. A Series of Isoreticular, Highly Stable, Porous Zirconium Oxide Based Metal–Organic Frameworks. *Angew. Chem., Int. Ed.* **2012**, *51* (37), 9267–9271.
- (20) Katz, M. J.; Brown, Z. J.; Colon, Y. J.; Siu, P. W.; Scheidt, K. A.; Snurr, R. Q.; Hupp, J. T.; Farha, O. K. A facile synthesis of UiO-66, UiO-67 and their derivatives. *Chem. Commun.* **2013**, *49* (82), 9449–9451.
- (21) Gui, B.; Meng, X.; Chen, Y.; Tian, J.; Liu, G.; Shen, C.; Zeller, M.; Yuan, D.; Wang, C. Reversible Tuning Hydroquinone/Quinone Reaction in Metal–Organic Framework: Immobilized Molecular Switches in Solid State. *Chem. Mater.* **2015**, *27* (18), 6426–6431.
- (22) Pan, L.; Parker, B.; Huang, X.; Olson, D. H.; Lee, J.; Li, J. Zn(tbip) (H2tbip= 5-tert-Butyl Isophthalic Acid): A Highly Stable Guest-Free Microporous Metal Organic Framework with Unique Gas Separation Capability. *J. Am. Chem. Soc.* **2006**, *128* (13), 4180–4181.
- (23) Cunha, D.; Gaudin, C.; Colinet, I.; Horcajada, P.; Maurin, G.; Serre, C. Rationalization of the entrapping of bioactive molecules into a series of functionalized porous zirconium terephthalate MOFs. *J. Mater. Chem. B* **2013**, *1* (8), 1101–1108.
- (24) Chen, T.-H.; Popov, I.; Kaveevivitchai, W.; Chuang, Y.-C.; Chen, Y.-S.; Daugulis, O.; Jacobson, A. J.; Miljanić, O. Š., Thermally robust and porous noncovalent organic framework with high affinity for fluorocarbons and CFCs. *Nat. Commun.* **2014**, *5*. DOI: 10.1038/ncomms6131
- (25) Miguet, M.; Goetz, V.; Plantard, G.; Jaeger, Y. Removal of a Chlorinated Volatile Organic Compound (Perchloroethylene) from the Aqueous Phase by Adsorption on Activated Carbon. *Ind. Eng. Chem. Res.* **2015**, *54* (40), 9813–9823.
- (26) Hayden, N. J.; Brooks, M. C.; Annable, M. D.; Zhou, H. Activated Carbon for Removing Tetrachloroethylene from Alcohol Solutions. *J. Environ. Eng.* **2001**, *127* (12), 1116–1123.
- (27) Wang, H.; Dong, X.; Velasco, E.; Olson, D. H.; Han, Y.; Li, J. One-of-a-kind: a microporous metal–organic framework capable of adsorptive separation of linear, mono- and di-branched alkane isomers via temperature- and adsorbate-dependent molecular sieving. *Energy Environ. Sci.* **2018**, *11* (5), 1226–1231.
- (28) Guillelot, M.; Mijoin, J.; Mignard, S.; Magnoux, P. Adsorption of Tetrachloroethylene on Cationic X and Y Zeolites: Influence of Cation Nature and of Water Vapor. *Ind. Eng. Chem. Res.* **2007**, *46* (13), 4614–4620.
- (29) Jeffroy, M.; Weber, G.; Hostachy, S.; Bellat, J.-P.; Fuchs, A. H.; Boutin, A. Structural Changes in Nanoporous MFI Zeolites Induced by Tetrachloroethene Adsorption: A Joint Experimental and Simulation Study. *J. Phys. Chem. C* **2011**, *115* (10), 3854–3865.
- (30) Webb, J. D.; Seki, T.; Goldston, J. F.; Pruski, M.; Crudden, C. M. Selective functionalization of the mesopores of SBA-15. *Microporous Mesoporous Mater.* **2015**, *203*, 123–131.
- (31) Lee, J. W.; Lee, J. W.; Shim, W. G.; Suh, S. H.; Moon, H. Adsorption of Chlorinated Volatile Organic Compounds on MCM-48. *J. Chem. Eng. Data* **2003**, *48* (2), 381–387.